bands at high pressures, both of which give the same magnitude of shift with pressure (Figure 3); these shifts are large, and it is suggested that a librational mode is included in this feature.[13] Since all the skeletal modes involving Zn–Cl bond stretches and Zn–Cl bending modes, as well as the pyridine ring rotational modes, would be expected to undergo changes at higher pressures, it is difficult to assign the lattice and skeletal modes in the higher pressure phase. Frequency shifts of the lattice modes with pressure are usually large,[20] and it can therefore be assumed that vibrations at low wavenumbers have now moved into the frequency range observable by the instrument used, thus further complicating the low-frequency spectrum. At this stage thus, no assignment in this region can be given.

Conclusion

The application of pressure on a hydrogen-bonded compound usually results in an increase in the hydrogen-bonded contacts.[20] This should cause the C–H and Zn–Cl stretching modes to shift downward, since they are weakened by the increasing strength of the H---Cl bond. This however has been found not to be the case for $ZnCl_2(py)_2$, as the stretching modes shift upward. The Zn–Cl bond length is thus shortened, resulting in higher frequency Zn–Cl stretching modes. Similarly, a reduction of H bonding resulted in shorter C–H bond lengths and lower frequency C–H bending vibrations. Since these are the only internal pyridine vibrations that undergo any dramatic changes at the phase transition, it is thought that a rotation about the Zn–N bond takes place above 10 kbar with a corresponding reduction in the Cl---H nonbonded interactions. If the phase transition does indeed primarily involve a change in the strength of the hydrogen bonds, the profound effect that moisture has on the transition pressure, as mentioned earlier, can easily be understood. Finally, the Zn(II) ion was found to be too small to form the polymeric octahedral structure, even up to pressures of 30 kbar.

Acknowledgment. We thank the University of Pretoria and the CSIR, Pretoria, for financial assistance.

Registry No. $ZnCl_2(py)_2$, 6843-20-5.

Supplementary Material Available: Tables of the wavenumbers and pressure dependence of the lattice modes and the internal pyridine modes of $ZnCl_2(py)_2$ (2 pages). Ordering information is given on any current masthead page.

Contribution No. 7454 from the Arthur Amos Noyes Laboratory, California Institute of Technology, Pasadena, California 91125

Electronic and Vibrational Spectra of $Ru_2(carboxylate)_4^+$ Complexes. Characterization of a High-Spin Metal–Metal Ground State

Vincent M. Miskowski,* Thomas M. Loehr,† and Harry B. Gray*

Received August 7, 1986

Solid-state near-infrared absorption spectra at low temperature have been obtained for eight compounds containing [Ru_2(carboxylate)$_4$X] chains or [Ru_2(carboxylate)$_4X_2$]$^-$ units (carboxylate is acetate, propionate, or *n*-butyrate), including single-crystal data for six compounds. The $\delta \rightarrow \delta^*$ transition is assigned to a band with a completely molecular *z*-polarized origin near 9000 cm^{-1}. Sharp vibronic structure has been interpreted with the aid of detailed vibrational studies. Butyrates show predominant *z*-polarized structure in an excited-state $\nu(Ru_2)$ of ~300 cm^{-1}, along with weak vibronic origins built on a_{1g} ν(RuO) at 430 cm^{-1} and $\delta(CO_2)$ at ~700 cm^{-1}. Propionates are similar, but ν(RuO) is at ~400 cm^{-1}, whereas acetates show strong progressions in both $\nu(Ru_2)$ and ν(RuO), the latter at ~360 cm^{-1}. The unusual vibronic effect is attributed to strong ground-state coupling of the a_{1g} ν(RuO) and $\nu(Ru_2)$ modes in the acetates. Weak, *x*,*y*-polarized absorption is observed for all compounds built on e_g vibronic origins at ~250 cm^{-1} ($\delta(RuO_2)$), ~310 cm^{-1} (ν(RuO)), and ~1450 cm^{-1} (symmetric $\nu(CO_2)$). Franck–Condon factors for progressions in a_{1g} modes built on the e_g vibronic origins are very different from those in the *z*-polarized spectrum. A very weak ($\epsilon \sim 1$–5) absorption with an electronic origin at ~6900 cm^{-1}, which exhibits molecular *x*,*y* polarization and a single long progression in $\nu(Ru_2)$ (~340 cm^{-1}), is assigned to the spin-forbidden $\pi^* \rightarrow \delta^*$ transition. In addition, two very weak and narrow peaks at 5048 (observed in absorption for one compound) and ~1600 cm^{-1} (observed in resonance Raman) are tentatively assigned to spin-flip transitions within the $(\pi^*,\delta^*)^3$ configuration.

Molecules containing metal–metal quadruple bonds often exhibit vibronic structure in the $\delta \rightarrow \delta^*$ absorption system.[1-3] The study of these systems is of great interest, because the vibronic structure contains considerable information about the metal–metal interaction. Particularly for carboxylate-bridged metal dimers, this interaction is not simply described.[4]

The diruthenium(II,III) carboxylates, $Ru_2(O_2CR)_4^+$, have a spin-quartet ground state.[5] Norman and co-workers[4] explained this ground state in terms of the pattern of metal–metal-bonding and -antibonding orbitals characteristic of strong metal–metal interactions. The diruthenium(II,III) compounds possess 3 electrons in excess of the 8 required for a metal–metal quadruple bond. The lowest energy metal–metal-antibonding orbitals, π^* and δ^*, turn out to be nearly degenerate. Thus, a high-spin $\sigma^2\pi^4\delta^2(\delta^*)^1(\pi^*)^2$ ground state is adopted.

Complexes with this ground state should display all of the electronic transitions characteristic of quadruply bonded dimers, including the $\delta \rightarrow \delta^*$ transition. Our investigation of this transition has centered mainly on the $Ru_2(O_2CR)_4X$ (X = halide) compounds, because in these chain-structured materials the chromophore orientation is often exceptionally favorable for single-crystal polarized electronic spectroscopy. We have found well-resolved vibronic structure in the $\delta \rightarrow \delta^*$ absorption systems of several $Ru(O_2CR)_4^+$ species, and it has been interpreted with the aid of ground-state vibrational spectroscopic studies.

† Oregon Graduate Center, Beaverton, OR 96006.

(1) (a) Trogler, W. C.; Gray, H. B. *Acc. Chem. Res.* **1978**, *11*, 232. (b) Hopkins, M. D.; Gray, H. B. *J. Am. Chem. Soc.* **1984**, *106*, 2468.
(2) (a) Martin, D. S.; Newman, R. A.; Fanwick, P. E. *Inorg. Chem.* **1979**, *18*, 2511. (b) Martin, D. S.; Newman, R. A.; Fanwick, P. E. *Inorg. Chem.* **1982**, *21*, 3400. (c) Huang, H. W.; Martin, D. S. *Inorg. Chem.* **1985**, *24*, 96.
(3) (a) Cotton, F. A.; Walton, R. A. *Multiple Bonds Between Metal Atoms*; Wiley: New York, 1982; Chapter 8. (b) Cotton, F. A.; Fanwick, P. E.; Gage, L. D. *J. Am. Chem. Soc.* **1980**, *102*, 1570.
(4) (a) Norman, J. G., Jr.; Kolari, H. J.; Gray, H. B.; Trogler, W. C. *Inorg. Chem.* **1977**, *16*, 987. (b) Norman, J. G., Jr.; Kolari, H. J. *J. Am. Chem. Soc.* **1978**, *100*, 791. (c) Norman, J. G., Jr.; Renzoni, G. E.; Case, D. A. *J. Am. Chem. Soc.* **1979**, *101*, 5256.
(5) (a) Stephenson, T. A.; Wilkinson, G. *J. Inorg. Nucl. Chem.* **1966**, *28*, 2285. (b) Mitchell, R. W.; Spencer, A.; Wilkinson, G. *J. Chem. Soc., Dalton Trans.* **1973**, 846.

0020-1669/87/1326-1098$01.50/0

A second interesting property of a $(\pi^*,\delta^*)^3$ quartet ground state is that there are spin-forbidden transitions to doublet states with the same electronic configuration (spin-flip transitions). Some very weak features at relatively low energies in the spectra of the diruthenium(II,III) carboxylates are attributable to these spin flips, as discussed herein.

Experimental Section

The compounds $Ru_2(AcO)_4Cl$,[5] Ru_2Prop_4Cl,[5] Ru_2But_4Cl,[5] $Cs[Ru_2(AcO)_4Cl_2]$,[6] $Ru_2(AcO)_4Br$,[7] and Ru_2Form_4Cl[7] were prepared by literature methods (AcO is acetate; Prop is propionate; But is *n*-butyrate; Form is formate). All compounds analyzed for the indicated formulations. Below we listed detailed preparation conditions for compounds investigated by single-crystal methods, including two new compounds.

Large tetragonal needles, up to several centimeters in length, of the $I\bar{4}2d$ form of Ru_2But_4Cl were obtained by overnight cooling of hot saturated solutions of crude material[5] in *n*-butyric acid. Lattice constants measured by X-ray photographic methods agreed with those of Cotton et al.,[8] and the tetragonal *c* axis was established as the needle axis. For comparison to the other crystal form (vide infra) an elemental analysis was obtained for a sample of large single crystals that had been carefully cleaned of adhering material under a microscope. Anal. Calcd (found): C, 32.8 (32.7); H, 4.82 (4.60); N, 0.00 (0.00). Flat pieces, a few millimeters long, of very large crystals were broken off and used for single-crystal absorption spectra. They were polished with fine alumina powder to appropriate thickness. Thin crystals showed a pronounced dichroism, dark red perpendicular to *c* and pale purple-pink parallel to c.

We have found that Ru_2But_4Cl crystallizes from CH_3OH or CH_3CN predominantly as a different tetragonal polymorph. The best crystals, obtained by slow evaporation of a dry CH_3CN solution, consisted of dendritic aggregates of large (up to 1 × 1 cm) square flat plates. Individual crystals showed a beautiful uniaxial cross optical figure under crossed polarizers and a uniform light blue-gray color but ground to a red-brown powder. Precession and Weissenberg X-ray photographs of a representative crystal showed Laue symmetry $4/m$ (*c* axis perpendicular to the well-developed face) and systematic absences consistent with any of the three body-centered space groups $I4$, $I\bar{4}$, and $I4/m$. We estimated $a = b = 12.0$ Å and $c = 7.4$ Å; the measured density (flotation in iodobenzene/CCl_4) was 1.82 ± 0.02 g/cm^3 vs. 1.83 g/cm^3 calculated for $Z = 2$. An elemental analysis of a sample of carefully selected and cleaned single crystals confirmed the near absence of solvent. Anal. Calcd (found): C, 32.8 (33.5); H, 4.82 (4.68); N, 0.00 (0.08).

The space group information implies a linear chain, $(Ru_2Cl)_\infty$, parallel to the *c* axis. In view of the extensive structural data available for ruthenium carboxylates[6,8-10] and, particularly, the isomorphism to the Ru_2Prop_4Cl structure,[6,9] a structure determination did not seem called for. However, we were able to confirm the chains parallel to *c* by means of a one-dimensional Patterson synthesis based on visually estimated (00*l*) photographic intensities,[11] $l = 1$–6. The strong intensity variation in these reflections yielded a RuRu distance, based on the assumed structure, of 2.27 ± 0.03 Å, in good agreement with that seen in other structures.[6,8-10] Since there is some ambiguity remaining as to the precise space group, we will refer to this polymorph of Ru_2But_4Cl by its Laue symmetry, $4/m$.

Axial absorption spectra of this $4/m$ form were easily obtained from the axial plate crystals. Considerable effort was devoted to obtaining σ/π spectra, that is, spectra for faces containing the *c* axis. We eventually found that evaporation of concentrated CH_3CN solutions of Ru_2But_4Cl onto quartz disks gave, reproducibly, some very thin crystals exhibiting a strong dark red–blue-gray dichroism. Most of these crystals developed fine parallel cracks (hence, light leaks) upon evaporation of the last solvent; most crystals that did not crack did not survive subsequent manipulation. However, by sheer persistence we eventually obtained high-quality data for several crystals.

We should note that the $I\bar{4}2d$ and $4/m$ polymorphs have readily distinguishable near-infrared vibronic absorption spectra, as indicated in the text. By this sensitive criterion, crude Ru_2But_4Cl obtained by us via the Wilkinson preparation[5] invariably was a mixture of the two polymorphs, according to low-temperature KBr pellet absorption spectra, with the $I\bar{4}2d$ form predominating. Microscopic inspection of recrystallized samples (independent of recrystallization solvent) also gave evidence for crystals of both forms. Thus, we advise caution in the interpretation of measurements on bulk samples of Ru_2But_4Cl. All data reported in this paper were obtained from carefully separated samples of large single crystals.

The new compound Ru_2But_4Br was obtained by addition of a few drops of saturated aqueous LiBr to a concentrated methanol solution of Ru_2But_4Cl. When the mixture was allowed to stand in air for a few days, crystals formed, the most common form being a flattened tetragonal prism. Anal. Calcd (found): C, 30.5 (30.7); H, 4.48 (4.35). X-ray photographic data indicated an isomorphism with the $4/m$ form of Ru_2But_4Cl, with $a = b = 12.0$ Å and $c = 7.6$ Å. The measured density (flotation in $CCl_4/CHBr_3$) was 1.90 ± 0.01 g/cm^3, vs. 1.90 g/cm^3 calculated for $Z = 2$.

Crystals were polished to yield axial faces, which showed well-developed uniaxial cross optical figures and a uniform light green color. We were unable to obtain σ/π crystal faces.

Crystals of Ru_2Prop_4Cl were initially obtained as described previously.[6] Crystallization from methanol with a few drops of saturated aqueous LiCl was found to yield larger crystals. The crystal structure is the $4/m$ form described above for Ru_2But_4X. It was originally refined in $I\bar{4}$[6] but has been shown[9] to be better described in $I4/m$, with disordered ethyl groups. The crystal morphology was a flattened tetragonal prism; crystals were polished to yield axial faces, with uniaxial cross optical figures and uniform light purple colors. We note that samples of Ru_2Prop_4Cl prepared from propionic acid[5] have a distinctly different appearance under a microscope, consisting of very fine red-brown needles, and it is possible that the propionate may, like the butyrate and acetate,[10] exhibit polymorphism.

The compound $[TBA][Ru_2Prop_4Br_2]$, where TBA is tetra-*n*-butylammonium, is representative of a large class of similar compounds prepared by us with tetraalkylammonium halides, and was selected for detailed study because its crystals showed a pronounced dichroism. Large crystals were grown as follows: Ru_2Prop_4Cl was dissolved in CH_3CN/0.1 M [TBA]Br. Evaporation of this solution yielded a gel in which orange crystals grew, when the gel was kept loosely covered for 1 week. When the bulk [TBA]Br had begun to crystallize, water was added, and the slurry was filtered and washed with copious amounts of water. The crystalline orange solid remaining on the frit was vacuum-dried. Anal. Calcd (found): C, 37.5 (38.7); H, 6.29 (6.48); N, 1.56 (1.91). Crystals were very thin blades that showed sharp (wavelength-independent) extinctions parallel and perpendicular to the long crystal axis, with associated colors of dark orange-red and light orange. The optical figure was an off-center biaxial optic axis one. Crystallographic characterization of this material was not pursued.

We have expended more effort in attempts to obtain crystals of $Ru_2(AcO)_4Cl$ (or its hydrate[6] $Ru_2(AcO)_4Cl\cdot 2H_2O$) than any of the other compounds in this study. We have irreproducibly obtained small dark red–light violet dichroic plates[10a] by slow evaporation from anhydrous methanol. We were unable to improve crystal formation by incorporating any of the following items in the solvent: acetic acid, acetic anhydride, water, LiCl. Most large crystals were twinned. Neither the hydrate[6] nor the other polymorph[10b] of $Ru_2(AcO)_4Cl$ yielded suitable crystals in our hands.

While we were able to duplicate the polarized visible absorption data of Martin et al.[10a] with many crystals, obtaining a crystal large enough for single-crystal near-infrared experiments proved to be very difficult. We report here data of somewhat marginal quality obtained for a crystal of maximal dimension of 0.3 mm. Our isotropic (pellet and mull) absorption spectra accord with the crystal results, so we assume that the bulk material (Wilkinson preparation[5]) is the same ($I2/m$) polymorph.

In general, polarized single-crystal electronic spectra employed previously described[12] equipment and techniques. Since the PbS near-infrared detector in our Cary 17 instrument is much less sensitive than our visible detectors, however, the use of large crystals is critical. In particular, because the detector sensitivity decreases rapidly for wavelengths less than 1000 nm, we frequently encountered artifactually rising base lines as a result of slit widths becoming comparable to crystal widths. For most compounds we eventually obtained crystals large enough so that such artifacts could be avoided by use of small slit widths; insensitivity of absorbance to slit program setting provides a sensitive test for artifacts. Most of the data in this paper show rather high noise levels; in general, we ran spectra at the largest time-constant settings of the instrument, and the noise levels thus reflect the smallest ones obtainable at the required slit widths without computer averaging.

Infrared and Raman spectra were obtained as described previously.[12]

(6) Bino, A.; Cotton, F. A.; Felthouse, T. R. *Inorg. Chem.* **1979**, *18*, 2599.
(7) Mukaida, M.; Nomura, T.; Ishimori, T. *Bull. Chem. Soc. Jpn.* **1972**, *45*, 2143.
(8) Bennett, M. J.; Caulton, K. G.; Cotton, F. A. *Inorg. Chem.* **1969**, *8*, 1.
(9) Marsh, R. E.; Schomaker, V. *Inorg. Chem.* **1981**, *20*, 299.
(10) (a) Martin, D. S.; Newman, R. A.; Vlasnik, L. M. *Inorg. Chem.* **1980**, *19*, 3404. (b) Togano, T.; Mukaida, M.; Nomura, T. *Bull. Chem. Soc. Jpn.* **1980**, *53*, 2085.
(11) We thank R. E. Marsh for suggesting this procedure and for guiding us through it.
(12) Miskowski, V. M.; Smith, T. P.; Loehr, T. M.; Gray, H. B. *J. Am. Chem. Soc.* **1985**, *107*, 7965.

Table I. Raman Data (cm^{-1}) for Solid Samples of Ruthenium Carboxylates at Room Temperature (647.1- or 676.4-nm Excitation)

compd	Raman data				
	a_{1g} $\nu(Ru_2)$	a_{1g} $\nu(RuX)$	a_{1g} $\nu(RuO)$	a_{1g} $\delta(Ru_2O)$	other lines
$Ru_2(AcO)_4Cl$	326 (330.1)[a]	159	370 (372.1)	187 (182.5)	295 (304), 173
$Ru_2(AcO_4)Br$	321	[b]	370	194	174, 108
Ru_2Prop_4Cl	336 (339.3)	160	405 (397.2)	183	(312.8)
$[TBA][Ru_2Prop_4Br_2]$	325	80	400	175	
Ru_2But_4Cl ($I\bar{4}2d$)	328 (332.6)	140	~440	177	~380 (379.6), (311), 250
Ru_2But_4Cl ($4/m$)	328	139	435	183	
Ru_2But_4Br	329	[b]	433	184	

[a] Low-temperature (80 K) data from ref 18b are given in parentheses. [b] Not observed.

Structural Considerations and the Effect of Carboxylate R Group Variation

Structural data for $Ru_2(O_2CR)_4Cl$ and $[Ru_2(O_2CR)_4Cl_2]^-$ show[6,8-10] RuRu distances in the range 2.267–2.286 Å, consistent[3a,13] with a formal metal–metal bond order of $2^1/_2$. Ruthenium–chloride bond distances of 2.517–2.587 Å are quite long but not exceptionally so for ligands trans to a strong metal–metal bond.[14,15]

Ruthenium–oxygen(carboxylate) bond lengths are 2.00–2.02 Å and RuRuO angles are all within a degree of 90°. The latter fact implies that RuO and RuRu vectors are nearly orthogonal. Importantly, variations of carboxylate R groups among methyl, ethyl, and *n*-propyl do not produce significant changes in any bond lengths or angles of the ruthenium complexes; nor are any evident in data for binuclear carboxylate complexes of other metal ions.[15]

Electrochemical measurements[16] on $Rh_2(O_2CR)_4$ show that the AcO, Prop, and But complexes are oxidized reversibly at potentials within 10 mV of each other. An irreversible reduction is similarly invariant. This is a nontrivial result, because these potentials can be varied over a range of ±0.5 V by larger variations in R.[16] It is reasonable to conclude, therefore, that the AcO, Prop, and But complexes with similar axial ligands are all electronically equivalent.

State Designations and Spin–Orbit Effects

Assuming D_{4h} symmetry, the $(\pi^*,\delta^*)^3$ configuration of $Ru_2(O_2CR)_4^+$ gives rise to a single quartet state, $^4B_{2u}$, and six doublet states. The former is the ground state if the π^*–δ^* one-electron splitting is sufficiently small. The close analogy to the low-lying states of a mononuclear octahedral d^3 complex is obvious.

We now briefly consider the effects of spin–orbit coupling. The D_{4h} double group has but four representations for half-integral spin, the Kramers doublets $E_{1/2}$ and $E_{3/2}$, which may be gerade or ungerade. Thus, the $^4B_{2u}$ ground state is split into $E_{1/2u}$ and $E_{3/2u}$ states separated by the zero-field splitting, $2D$. The LaPorte selection rule remains rigorous, but $E_{1/2u} \leftrightarrow E_{1/2g}$ and $E_{3/2u} \leftrightarrow E_{3/2g}$ transitions are both formally allowed both z and x,y, whereas $E_{1/2u} \leftrightarrow E_{3/2g}$ and $E_{3/2u} \leftrightarrow E_{1/2g}$ are allowed only x,y. Thus, in principle, spin–orbit coupling provides a mechanism for mixing z- and x,y-allowed transitions with each other and with orbitally forbidden (but LaPorte-allowed) transitions. We have considered the possibility of such effects in our data, but have seen no evidence of it.

Now, consider the $\delta \rightarrow \delta^*$ transition ($^4B_{2u} \rightarrow {}^4B_{1g}$), which is formally z-dipole allowed. Assuming negligible x,y intensity, the pure electronic transition consists of two z-polarized lines, $E_{1/2u}(^4B_{2u}) \rightarrow E_{1/2g}(^4B_{1g})$ and $E_{3/2u}(^4B_{2u}) \rightarrow E_{3/2g}(^4B_{1g})$. The splitting of these two lines should depend on the zero-field splittings of both ground and excited states.

The zero-field splitting ($2D$) has been estimated[17b] to be 154 cm^{-1}, with $E_{1/2u}$ lowest, for the $I\bar{4}2d$ form of Ru_2But_4Cl. Less detailed magnetic studies of other ruthenium carboxylates[5a,7] suggest that the Ru_2But_4Cl results[17] should be representative for this class of compounds.

Table II. Far-Infrared Data (cm^{-1}) for Ruthenium Carboxylates

compd	far-IR data			
	ν(RuO)		ν(RuX)	
	e_u	a_{2u}	a_{2u}	other lines
$Ru_2(AcO)_4Cl$	405	341	204	248, 189, 159, 124, 90
$Ru_2(AcO)_4Br$	403	349	137	255, 191, 130, 58
$Cs[Ru_2(AcO)_4Cl_2]$	396	343	211	250, 177, 120
Ru_2Prop_4Cl	425	351	200	230
$TBA[Ru_2Prop_4Br_2]$	427	352	128	250, 200, 71
Ru_2But_4Cl ($I\bar{4}2d$)	457	343	185	280, 150, 112
Ru_2But_4Cl ($4/m$)	456	343	188	280, 142, 108
Ru_2But_4Br	453	342	125	188

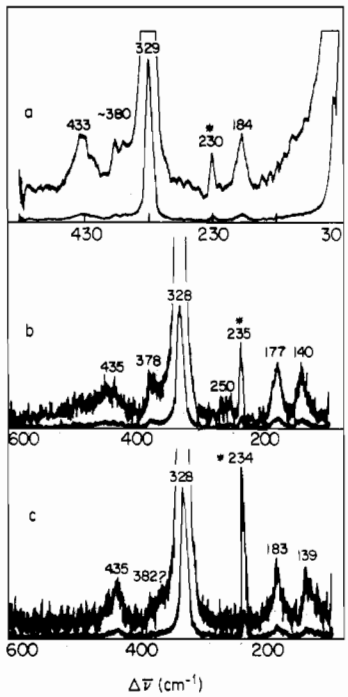

Figure 1. Raman spectra of solid samples: (a) Ru_2But_4Br, 676.4-nm excitation; (b) $I\bar{4}2d$ polymorph of Ru_2But_4Cl, 647.1-nm excitation; (c) $4/m$ polymorph of Ru_2But_4Cl, 647.1-nm excitation. Plasma lines are indicated by asterisks. Spectral slit widths for all spectra were ~7 cm^{-1}.

At sufficiently low temperatures, only the $E_{1/2u} \rightarrow E_{1/2g}$ transition will be observed, whereas $E_{3/2u} \rightarrow E_{3/2g}$ should appear at higher temperatures. We did not observe any lines attributable to the latter growing in at higher temperatures, but severe thermal line broadening above ~100 K probably obscured the expected effects.

Vibrational Spectra

It will prove to be crucial to our electronic spectral interpretation to have good assignments for fundamental vibrations of a_{1g} and e_g symmetry (D_{4h} labels); in this section, we report Raman and infrared spectral results. Our task for Raman spectra is to supplement the extensive studies of Clark and co-workers[18] with more

(13) Bino, A.; Cotton, F. A. *Inorg. Chem.* **1979**, *18*, 3562.
(14) Collins, D. M.; Cotton, F. A.; Gage, L. D. *Inorg. Chem.* **1979**, *18*, 1712.
(15) Koh, Y. B.; Christoph, G. G. *Inorg. Chem.* **1979**, *18*, 1122.
(16) Das, K.; Kadish, K. M.; Bear, J. L. *Inorg. Chem.* **1978**, *17*, 930.
(17) (a) Cotton, F. A.; Pedersen, E. *Inorg. Chem.* **1975**, *14*, 388. (b) Telser, J.; Drago, R. S. *Inorg. Chem.* **1984**, *23*, 3114.

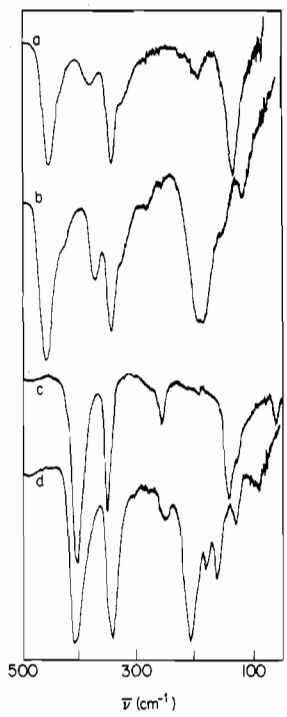

Figure 2. Far infrared spectra (hydrocarbon mulls between polyethylene plates) of solid samples: (a) Ru_2But_4Br; (b) $I\bar{4}2d$ polymorph of Ru_2But_4Cl; (c) $Ru_2(AcO)_4Br$; (d) $Ru_2(AcO)_4Cl$.

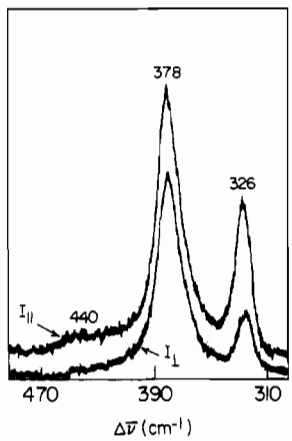

Figure 3. Polarized[21] Raman spectra (647.1-nm excitation) for 5×10^{-3} M $[Ru_2But_4Br_2]^-$ in CH_3CN (0.1 M [TBA]Br) solution. The depolarized line at 378 cm^{-1} is due to CH_3CN.

attention given to some of the weaker Raman lines. Since we are interested in fundamentals, we have concentrated on preresonance Raman excitation, where overtone enhancement is insignificant. We have also measured far-infrared spectra[17b,18a] as an aid in interpreting the Raman data.

Data are summarized in Tables I and II, and selected spectra are displayed in Figures 1–3. Details of assignments in the tables are discussed below. Where room-temperature data have been obtained by both Clark et al.[18] and us, frequency agreement is close except for some of the weakest lines, where differences in data treatment may be responsible. In these cases we give our own values for consistency.

Metal–Metal and Metal–Halide Stretches

For a D_{4h} $[Ru_2(O_2CR)_4X_2]^-$ unit, there are two a_{1g} modes corresponding to RuRu and RuX stretching, and an a_{2u} RuX stretching mode. Strictly analogous modes exist for a symmetric infinite chain $[Ru_2(O_2CR)_4X]_\infty$. The a_{1g} $\nu(Ru_2)$ mode has been assigned by Clark et al. for $Ru_2(O_2CR)_4Cl$ compounds; for all

(18) (a) Clark, R. J. H.; Franks, M. L. *J. Chem. Soc., Dalton Trans.* **1976**, 1825. (b) Clark, R. J. H.; Ferris, L. T. H. *Inorg. Chem.* **1981**, *20*, 2759.

Table III. Raman Data (cm^{-1}) for $Ru_2But_4^+$ Complexes in CH_3CN Solution[a]

complex	excitation λ = 488 nm	excitation λ = 647.1 nm	depolarization ratio	assignt
$Ru_2But_4Cl(CH_3CN)$[b]		177 (vw)		$\delta(Ru_2O)$
	334	335	0.50	$\nu(Ru_2)$
	668			$2\nu(Ru_2)$
	1001			$3\nu(Ru_2)$
$[Ru_2But_4Cl_2]^-$[c]		175 (vw)		$\delta(Ru_2O)$
	333	332	0.50	$\nu(Ru_2)$
	666			$2\nu(Ru_2)$
	1000			$3\nu(Ru_2)$
$[Ru_2But_4Br_2]^-$[d]		174 (vw)		$\delta(Ru_2O)$
		260 (vw)		$\delta(RuO_2)$
	326	326	0.50	$\nu(Ru_2)$
		440 (w)	0.3	$\nu(RuO)$
	651.5			$2\nu(Ru_2)$
	974			$3\nu(Ru_2)$

[a] See ref 21. Depolarization ratios were determined for only the strongest lines. For 488-nm excitation, the intensity ratios for $3\nu(Ru_2)/2\nu(Ru_2)/\nu(Ru_2)$ were 0.1/0.4/1.0. The Raman spectrum for the dibromo complex was considerably stronger, relative to solvent lines, than that of the other complexes. [b] Ru_2But_4Cl in neat CH_3CN. [c] Ru_2But_4Cl in 0.1 M [TBA]Cl/CH_3CN. [d] Ru_2But_4Cl in 0.1 M [TBA]Br/CH_3CN.

but the acetate it is by far the strongest Raman line, and ^{18}O isotope-substitution data provided a definitive assignment for the acetate. Analogous assignments (Table I) follow readily for all of the other compounds of the present study, and place $\nu(Ru_2)$ in the narrow range 321–336 cm^{-1}.

Assignment of the a_{2u} ν(RuX) mode is confirmed by the shift of a very strong line near 200 cm^{-1} to ~140 cm^{-1} upon replacement of chloride by bromide (Figure 2). The a_{1g} ν(RuCl) mode is assigned to a line at ~150 cm^{-1} that disappears upon bromide substitution (Figure 1).

These assignments are reasonable according to one-dimensional XRuRuX force-field calculations.[19,20] Thus, the frequencies listed for $Ru_2(AcO)_4Cl$ yield $k(Ru_2)$ = 2.59, k(RuCl) = 0.64, and an off-diagonal force constant, k_{12}, of −0.035 mdyn/Å. With k_{12} assumed to be the same, the $Ru_2(AcO)_4Br$ data, lacking a_{1g} ν(RuBr), yield $k(Ru_2)$ = 2.67 and k(RuBr) = 0.49 mdyn/Å, with a_{1g} ν(RuBr) calculated at 96 cm^{-1}. No clearly defined Raman feature is observed near 100 cm^{-1} (see Figure 1a, for example) for bromides, except for $[TBA][Ru_2Prop_4Br_2]$, whose strong Raman line at 80 cm^{-1} is tentatively assigned to ν(RuBr) in Table I. Since the force-field model above neglects mixing with deformation and carboxylate modes, derived force constants are subject to systematic error, but their comparison to those obtained for other binuclear metal compounds with similar approximations (e.g., those of ref 20 for $Re_2(AcO)_4X_2$) is informative.

A final interesting point is that the depolarization ratios of $\nu(Ru_2)$ for the butyrates (Table III, Figure 3) are consistent[21] with a pure axial mode ($\alpha_{xx} = \alpha_{yy} \simeq 0$) both for resonance (488 nm) and preresonance (647.1 nm) excitation. As noted by Clark and Ferris,[18b] the former result follows necessarily from the axial (z) polarization of the resonant visible electronic transition. However, the latter finding suggests that $\nu(Ru_2)$ is actually a pure axial stretching mode, which would be anticipated[20] from the near-orthogonality of the Ru_2 and RuO stretching coordinates. Our observation contrasts with the marked polarization dispersion displayed[18b] by $\nu(Ru_2)$ of the acetate; there, an exceptionally small energy gap between the symmetric Ru/Ru and RuO modes (Table I) has evidently promoted mixing of the stretching coordinates,

(19) Herzberg, G. *Infrared and Raman Spectra of Polyatomic Molecules*; Van Nostrand: New York, 1945; pp 188–189.
(20) Bratton, W. K.; Cotton, F. A.; Debeau, M.; Walton, R. A. *J. Coord. Chem.* **1971**, *1*, 121.
(21) Theoretical depolarization ratios for our scattering geometry are 1/2 for single-axis- (z-) polarized lines, 0.285 for perpendicular- (x,y-) polarized lines, and 0.86 for depolarized lines.

as independently (and compellingly) indicated by the strong resonance enhancement[18] of ν(RuO).

Metal–Oxygen Stretches

In D_{4h} there are six RuO(carboxylate) stretching modes, transforming as $a_{1g} + b_{1g} + e_g + a_{2u} + b_{2u} + e_u$. Clark et al.[18] have assigned the a_{1g} mode to a resonance-enhanced Raman line. We agree with their assignment for acetates and propionates (Table I), but not for butyrates. As shown in Figure 1, our spectra of the $I\bar{4}2d$ form of Ru_2But_4Cl do show the weak line at ~380 cm^{-1} assigned previously[18] to the totally symmetric ν(RuO). However, we also see a line at ~440 cm^{-1}. For the $4/m$ form of Ru_2But_4Cl, the ~380-cm^{-1} feature is much weaker, whereas a sharp line at 435 cm^{-1} remains. We reassign the a_{1g} ν(RuO) to the 435-cm^{-1} line, and suggest that the ~380-cm^{-1} peak may be a nontotally symmetric ν(RuO) or, perhaps, an alkyl group deformation mode, whose intensity has been promoted by the low site symmetry of the $I\bar{4}2d$ crystal form.

Two lines of argument support this assignment. First, the intensity of ν(RuO) relative to $\nu(Ru_2)$ is lower than for the propionates (ν(RuO) ~400 cm^{-1}), and much lower than for the acetates. This is consistent with a larger splitting between these modes (less Ru_2 stretching character in ν(RuO)), according to the mixing mechanism suggested in the previous section. Secondly, Figure 3 shows that a ~440-cm^{-1} line of $[Ru_2But_4Br_2]^-$ in CH_3CN solution is strongly polarized, $\rho \sim 0.3$. This depolarization ratio is consistent[21] with assignment to an essentially equatorial ($\alpha_{zz} \sim 0$) totally symmetric mode.

In the case of acetates the lowest frequency[22] infrared-active ligand mode is a very weak CO_2 rock at ~480 cm^{-1}. We therefore assign the two strong lines of the acetates (Figure 2) at ~400 and ~340 cm^{-1} to the two expected infrared-active ν(RuO) modes, e_u and a_{2u}. The general appearance of the spectra and the assignments are very similar to those for rhodium(II)[25] and copper(II) acetates.[23,26] For butyrates, a moderately intense alkyl deformation mode occurs in the same spectral region:[24] we observe it at 355 and 364 cm^{-1}, respectively, for potassium butyrate and *n*-butyric acid, and assign the line of the ruthenium complexes at 370–380 cm^{-1} to the same mode. The ν(RuO) line at higher energy is assigned to the e_u mode, because it is consistently broader and more intense than the other line.

The very considerable variation of ν(RuO) values as a function of carboxylate R group was a surprise to us, as structural comparisons led us to anticipate virtually identical RuO force constants in all these compounds. However, the a_{2u} frequency is essentially independent of R group. If we consider a single carboxylate, the a_{2u} ν(RuO) mode has the two oxygens moving out of phase, while both a_{1g} and e_u have them moving in phase. The latter should result in a large rigid-body motion of the entire carboxylate unit relative to Ru_2; thus, we suspect that the frequency variation of these modes is essentially a mass (*G* matrix) effect. Accounting for observed frequency variations would require a detailed consideration of the coupling among all the various vibrational modes in the carboxylate–Ru_2 units, and we have not attempted force-field calculations of the required complexity. But we emphasize that the frequency variation is real and that it has the important consequence of affecting the coupling between the a_{1g} ν(RuO) and $\nu(Ru_2)$ modes.

Finally, we note that $Ru_2(AcO)_4Cl$ shows a weak Raman line at 295 cm^{-1} (room temperature) and one at 304 cm^{-1} (80 K). Clark et al.[18b] suggested that the line is attributable to $\nu(Ru_2)-\nu_L$, where ν_L is a lattice mode. However, since the line appears with similar intensity for preresonance excitation, whereas other overtones and combinations become very weak, we feel that an alternative assignment is appropriate. Importantly, Figure 2 of ref 18b clearly shows that at 80 K the weak line shifts from 304 to ~295 cm^{-1} for the [^{18}O]acetate derivative. This large isotope shift strongly supports a ν(RuO) assignment. Since the $Ru_2(AcO)_4Cl$ crystal structure[10] places the chromophores at inversion centers, a D_{4h} gerade mode, either b_{1g} or e_g, is required. Clark et al.[18b] report lines for Ru_2Prop_4Cl and Ru_2But_4Cl at, respectively, 312.8 and 311 cm^{-1} (80 K), and the assignments may be analogous.

Metal–Ligand Deformations

In D_{4h} there are a total of 10 RuO(carboxylate) deformations, including one a_{1g} mode and two e_g modes, plus two Ru–axial ligand deformations. We expect the former in the 300–100-cm^{-1} range and the latter to fall below 100 cm^{-1}. While many lines are evident in our data in the appropriate spectral region, detailed assignments are difficult.

All of the compounds show a Raman line near 180 cm^{-1}, and in many cases this is the only strong peak other than those already assigned; the line is probably the a_{1g} δ(RuRuO) umbrella mode. Unfortunately, we could not obtain accurate solution depolarization ratios for this feature, which might have confirmed (or disproved) the assignment.

The $I\bar{4}2d$ polymorph of Ru_2But_4Cl also shows a weak Raman line near 250 cm^{-1}, and some weak Raman features of similar frequency have been reported by Clark et al.[18] for other compounds. The frequency qualitatively suggests a deformation mode with a high degree of δ(ORuO) character, and comparison to the calculations of Cotton et al.[20] indicates that assignment to an e_g δ(ORuO) mode is reasonable.

Carboxylate Vibrational Modes

Structural compilations[15] show that the dimensions of the carboxylate CO_2 units are responsive to changes in metal–metal distances. Vibrational modes of these units, in particular the symmetric CO_2 bend and the symmetric and asymmetric CO_2 stretches, will now be considered: For $M_2(O_2CR)_4$, the first two yield $a_{1g} + b_{1g} + e_u$ modes, while the last yields $a_{2u} + b_{2u} + e_g$.

Unfortunately, the a_{1g} and e_g frequencies cannot be obtained from Raman spectra, because resonance effects make the ligand modes disproportionately weak relative to core vibrations. The only ligand mode assigned by Clark et al.[18] is "ν(CO)" at ~1600 cm^{-1}, which as discussed later, is probably not a vibrational transition.

For estimates of the CO_2 vibrational frequencies, we turn to the infrared spectra of the acetates, which are reasonably well understood[23,26,27] and should aid in the interpretation of the more complex spectra of the propionates and butyrates. Anhydrous $Cu_2(AcO)_4$ shows $\delta(CO_2)$ as an intense line in its IR spectrum at 691 cm^{-1}. The very similar IR spectrum of $Ru_2(AcO)_4Cl$ shows a strong line at 694 cm^{-1}. The a_{1g}, b_{1g}, and e_u splittings of $\delta(CO_2)$ can be estimated roughly from the reported data for $Mo_2(AcO)_4$.[20] The strong IR line at 675 cm^{-1} (presumably e_u) has strong Raman counterparts at 690 and 686 cm^{-1}, which probably are a_{1g} and b_{1g}.

$Ru_2(AcO)_4Cl$ has its most intense infrared absorption as a broad peak maximizing at ~1450 cm^{-1}, and an analogous band is observed in the spectrum[20] of $Re_2(AcO)_4Cl_2$. Both the asymmetric and symmetric $\nu(CO_2)$ modes, together with a CH_3 asymmetric deformation,[23] probably are included in this feature. Again, the spectrum of $Mo_2(AcO)_4$ is informative:[20] infrared features at 1510 and 1492 cm^{-1} are attributable to asymmetric $\nu(CO_2)$ vibrations, whereas strong Raman (1432) and infrared lines (1440 cm^{-1}) are assigned to symmetric $\nu(CO_2)$ modes. For the ruthenium complexes, we suggest that the asymmetric and symmetric modes are near the upper and lower limits[28] of the ~1500–1400-cm^{-1} range.

(22) Bands attributable to methyl torsional modes should occur at lower frequency. However, they are expected to be extremely weak and broad at room temperature: Durig, J. R.; Craven, S. M.; Harris, W. C. *Vib. Spectra Struct.* **1972**, *1*, 73.
(23) Heyns, A. M. *J. Mol. Struct.* **1972**, *11*, 93.
(24) Bentley, F. F.; Smithson, L. D.; Rozek, A. L. *Infrared Spectra and Characteristic Frequencies; ~700–300 cm^{-1}*; Wiley: New York, 1968.
(25) Miskowski, V. M.; Schaefer, W. P.; Sadeghi, B.; Santarsiero, B. D.; Gray, H. B. *Inorg. Chem.* **1984**, *23*, 1154.
(26) Mathey, Y.; Greig, D. R.; Shriver, D. F. *Inorg. Chem.* **1982**, *21*, 3409.
(27) Deacon, G. B.; Phillips. R. J. *Coord. Chem. Rev.* **1980**, *33*, 227.
(28) We have also measured the infrared spectrum of Ru_2Form_4Cl, which lacks interference from alkyl deformation modes. Strong features at 1503 and 1470 cm^{-1}, attributable to asymmetric and symmetric ν(CO) modes, respectively, are observed.

Table IV. Low-Temperature $\delta \rightarrow \delta^*$ Vibronic Absorption Data (cm^{-1}) for Ruthenium Butyrates and Propionates

	$4/m$ Ru_2But_4Cl	$4/m$ Ru_2But_4Br	$I\bar{4}2d$ Ru_2But_4Cl	$I4/m$ Ru_2Prop_4Cl	$[TBA][Ru_2Prop_4Br_2]$
electronic origin	8900	8885	8950 9000[a]	8990	8670
a_{1g} modes					
$\nu(Ru_2)$	305	305	302	~310	290
$\nu(RuO)$	432	432	428	*b*	393
$\delta(CO_2)$	695	703	690	*b*	*b*
other weak lines	65	50	110[c]		
	130	110	158		
	~180	175	217		
			260		
e_g modes					
$\delta(RuO_2)$	245	240	255	*b*	*b*
$\nu(RuO)$	310	310	310	~300	*b*
$\nu(CO_2)$	1450	1445	1470	~1450	1460

[a] Origin split by crystal factor group. [b] Not resolved. [c] Frequencies relative to the 8950-cm^{-1} origin line. These lines probably include at least two factor group split doublets.

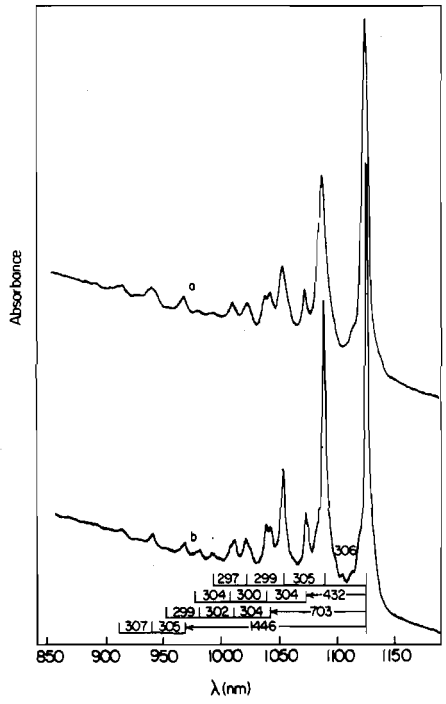

Figure 4. KBr pellet spectra (~2 mg/250 mg of KBr) at 15 K: (a) $4/m$ Ru_2But_4Cl; (b) $4/m$ Ru_2But_4Br.

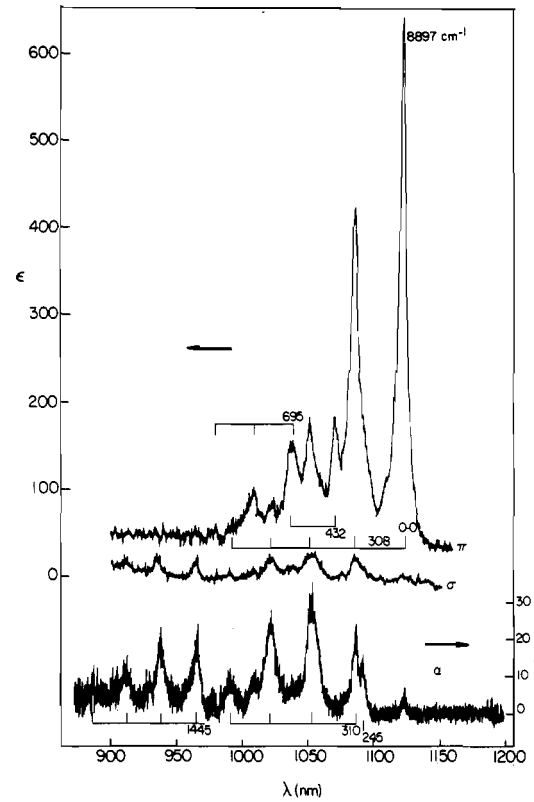

Figure 5. Polarized single-crystal spectra of $4/m$ Ru_2But_4Cl at 15 K. The axial (α) crystal was 30-μm thick and the σ/π crystal was 3.8-μm thick. The π spectrum is vertically offset by 40 ϵ units from the σ spectrum.

The anhydrous ruthenium compounds definitely do not show any strong infrared absorptions near 1600 cm^{-1}; this appears to be typical[27] of $M_2(O_2CR)_4$ complexes with short metal–metal bonds.

$\delta \rightarrow \delta^*$ Transition

The $\delta \rightarrow \delta^*$ transition of $Ru_2(O_2CR)_4^+$ complexes has been assigned by Norman et al.[4c] to a weak ($\epsilon \sim 25$–50 at room temperature[29]) band near 1000 nm, which was originally reported by Wilson and Taube.[30] The assignment was based on SCF–Xα–SW calculations, which are expected to give accurate predictions of the $\delta \rightarrow \delta^*$ transition energy in this case.[31,32]

The spectra of solid samples of all of the ruthenium compounds at room temperature show a broad band of shape, intensity, and energy similar to the solution absorption band.[30,32] At low temperature this band develops striking vibronic structure, as illustrated in Figure 4 for $4/m$ ruthenium butyrates. Polarized single-crystal spectra for $4/m$ Ru_2But_4Cl are shown in Figure 5. The axial (α) and perpendicular to c (σ) spectra are identical, which establishes that the absorptions are electric dipole transitions. The band is predominantly π polarized, which is equivalent to molecular z polarization for this crystal. Moreover, the lowest energy line at 1124 nm is completely z polarized.[33]

The z-polarized spectrum consists of a progression in a ~300-cm^{-1} frequency, along with two weaker progressions with origins displaced from the lowest energy line by ~430 and ~700 cm^{-1}.[34] Data for this and other complexes are summarized in Table IV.

Increasing the temperature results in the growth of a hot band ~330 cm^{-1} to the red of the lowest "cold" absorption line (Figure 6). This frequency and the temperature dependence are consistent

(29) Miskowski, V. M.; Gray, H. B, unpublished work.
(30) Wilson, C. R.; Taube, H. *Inorg. Chem.* **1975**, *14*, 2276.
(31) Noodleman, L.; Norman, J. G., Jr. *J. Chem. Phys.* **1979**, *70*, 4903.
(32) Hopkins, M. D.; Gray, H. B.; Miskowski, V. M. *Polyhedron*, in press.

(33) Very weak x,y intensities observed for the origin line in this and other data sets are well within those to be expected from crystal orientation errors.
(34) The ~700-cm^{-1} vibronic origin is not well defined in Figure 5, but it was well resolved in spectra of other crystals and of pellets (Figure 4). We chose Figure 5 for display because it includes our best resolved σ spectrum.

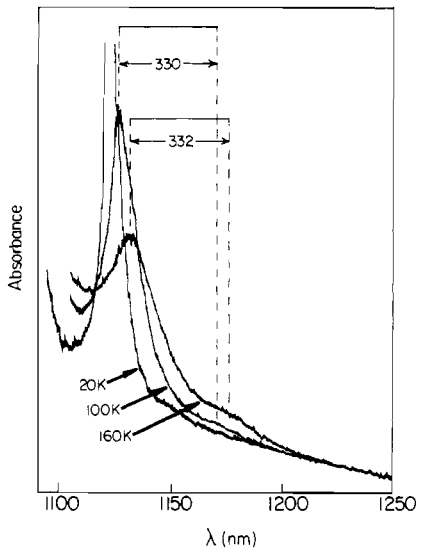

Figure 6. Temperature dependence of the 0–0 ($\delta \rightarrow \delta^*$) region for a KBr pellet of $4/m$ Ru_2But_4Cl.

with assignment of the hot band to $\nu(Ru_2)$, with the predominant 300-cm^{-1} progression frequency assigned to the excited-state $\nu(Ru_2)$. This behavior also indicates that the 1124-nm absorption line is a pure electronic (0–0) transition.

Pronounced thermal broadening also occurs (Figure 6), and a moment analysis[35] of the temperature dependence of both ν_{max} and the half-width of the origin line yields an effective frequency of $\sim$75 cm^{-1}. This frequency, which is not consistent with the ground-state zero-field splitting,[17b] most likely represents a ruthenium–halide deformation. At temperatures above 25 K, similarly, drastic thermal dependences were observed[3b] for the $\delta \rightarrow \delta^*$ absorption of the spin-doublet ground-state Tc_2(2-oxopyridinato)$_4$Cl, as well as for the other compounds under investigation here.

The x,y polarization (σ and α of Figure 5) shows a set of three progressions in a 300-cm^{-1} frequency: these are placed 245, 310, and 1450 cm^{-1} to higher energy of the 0–0 line. The progression built on the 1450-cm^{-1} origin is completely x,y polarized, but the situation is less well defined for the other features. The broad room-temperature absorption band of all the compounds is split[30] by $\sim$1500 cm^{-1}, and the temperature dependence shows that this splitting is related to the 1450-cm^{-1} low-temperature interval.

The isotropic and axial crystal $\delta \rightarrow \delta^*$ absorption bands of $4/m$ Ru_2But_4Br are nearly identical with those of $4/m$ Ru_2But_4Cl (Table IV). The same axial crystals gave very distinguishable visible electronic absorption spectra, however.[29] Isotropic and axial crystal spectra also were obtained for the $4/m$ ($I4/m$) crystals of Ru_2Prop_4Cl. Our observations (Table IV) are consistent with Figures 4 and 5, but much less informative, as the individual vibronic line widths were $\sim$200 cm^{-1} at low temperature. Thus, only the 300- and 1450-cm^{-1} intervals were resolved, but the z polarization of the origin was nevertheless established. The large line widths might be related to the crystal disorder observed by Marsh and Schomaker.[9]

We now turn to the $I\bar{4}2d$ polymorph of Ru_2But_4Cl. Polarized spectra (by far the highest quality spectra obtained in this study) are shown in Figure 7. The crystal structure[8] places the RuRu vector perpendicular to the c axis; the oriented gas approximation would then predict the $\|c$ spectrum to be pure molecular x,y, whereas $\sigma(\perp c)$ should be a 50/50 mixture of molecular x,y and molecular z. The spectra (Figure 7) are consistent with this prediction, translating from those of the $4/m$ polymorph (Figure 5), with the complication that every line shows a $\sim$50-cm^{-1} splitting into an unsymmetrical doublet. Note particularly the pure σ polarization of the origin lines, and the 2/1 π/σ intensity ratio of the progression based on the $\sim$1450-cm^{-1} interval.

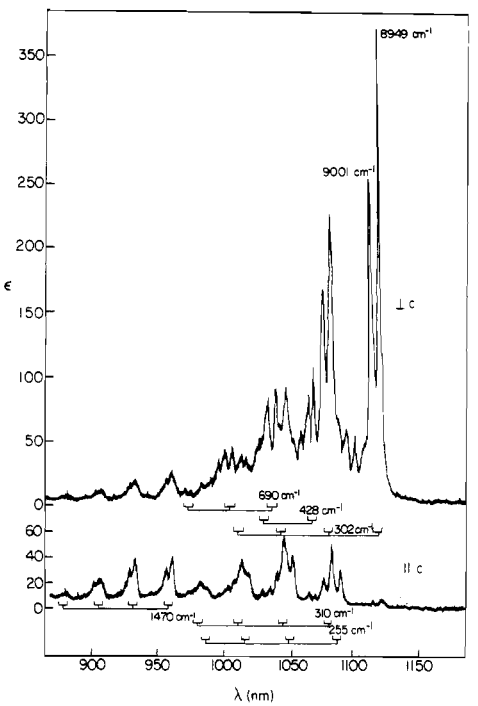

Figure 7. Polarized single-crystal spectra of $I\bar{4}2d$ Ru_2But_4Cl at 8 K. The crystal was 21-μm thick.

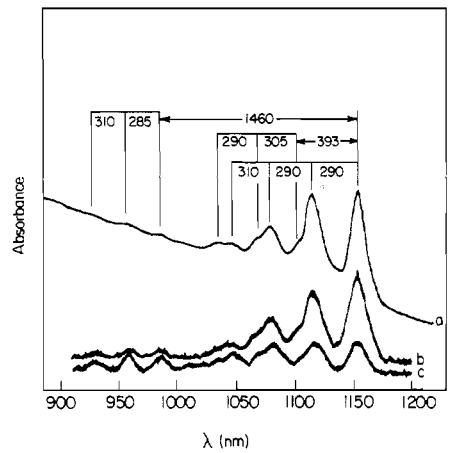

Figure 8. Spectra at 15 K for [TBA][$Ru_2Prop_4Br_2$]: (a) KBr pellet; (b) single crystal, strong extinction (dark orange color); (c) single crystal, weak extinction (light orange color).

The $\sim$50-cm^{-1} splitting is easily explained, given the fortunate circumstance that we have the spectral data of Figures 4 and 5 for another polymorph. The $I\bar{4}2d$ crystal form has $Z = 8$, or $Z = 4$ for the primitive cell. The Ru_2Cl units, forming *nonlinear* infinite chains, are in C_2 site positions oriented perpendicular to the crystal c axis. The crystal factor group (D_{2d}) predicts that a molecular z-polarized transition should yield two crystal $E(\perp c)$ transitions, and we assign the doublets accordingly. The $4/m$ polymorph has $Z = 1$ in the primitive cell, and therefore cannot show factor group splittings.

On a molecular basis, the splitting can be envisioned as arising from the nonlinear chains. The repeat unit[8] is sketched below.

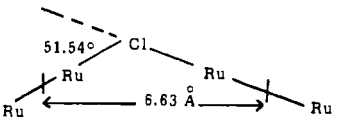

A simple dipole–dipole coupling (Davydov) model[36] would predict that the ratio of intensities (higher to lower energy) of

(35) Markham, J. J. *Rev. Mod. Phys.* **1959**, *31*, 956.

(36) Craig, D. P.; Walmsley, S. H. *Excitons in Molecular Crystals*; W. A. Benjamin: New York; 1968.

Table V. Low-Temperature $\delta \rightarrow \delta^*$ Vibronic Absorption Data (cm^{-1}) for Ruthenium Acetates in KX Pellets and/or Hydrocarbon Mulls

	$Ru_2(AcO)_4Cl$	$Ru_2(AcO)_4Br$	$[Ru_2(AcO)_4Br_2]^-$ in KBr	$[Ru_2(AcO)_4Cl_2]^-$ in KCl	$Cs[Ru_2(AcO)_4Cl_2]$
electronic origin	8945	8985	8735	8760[b]	8795
a_{1g} modes					
$\nu(Ru_2)$	295	290	295		285
$\nu(RuO)$	358	357	355		357
other weak lines	70		*a*		210
	180				
e_g modes					
$\delta(RuO_2)$	~230(?)				
$\nu(RuO)$	290				
$\nu(CO_2)$	1460	1462			

[a] Many weak lines were evident near the origin, but assignment to species other than $[Ru_2(AcO)_4Br_2]^-$ cannot be excluded. [b] A limiting spectrum for the reaction of $Ru_2(AcO)_4Cl$ with KCl was not obtained; only the origin is given.

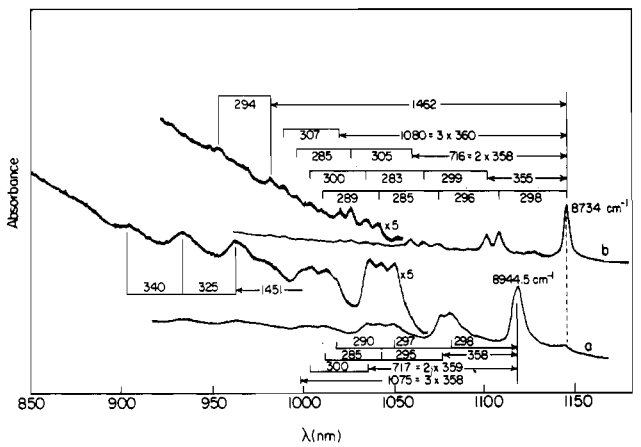

Figure 9. Spectra of KBr pellets of $Ru_2(AcO)_4Cl$ at 15 K: (a) spectrum after minimal exposure of compound to KBr; (b) spectrum after extensive regrinding and repressing of the pellet.

the two transitions should be $\tan^2(51.54°/2) = 0.23$, which only roughly accords[37] with observation. The failure of the simple model to account for quantitative features is not surprising, because the crystal is magnetic as well as ionic. Some of the complexities that can appear in a case of this sort have been treated for Cr_2O_3.[38]

The KBr pellet (isotropic) and single-crystal polarized spectra for $[TBA][Ru_2Prop_4Br_2]$ are shown in Figure 8. Although the crystal structure of this compound has not been determined, the polarization data can be interpreted because with very thin crystals we found a strong extinction/weak extinction intensity ratio of ~2 for the intense 480-nm band.[39] As this band is known to be molecular *z* polarized,[10,18b] the similar polarization ratio for the origin line (Figure 8) also indicates molecular *z* polarization. The vibronic patterns in these spectra also accord with our other data. Thus, it appears that these patterns are characteristic of $Ru_2(O_2CR)_4^+$ and that they are not perturbed significantly when this chromophore resides in a chain structure.

Unlike propionates and butyrates, the ruthenium acetates were found to react with alkali-metal halide matrices. Extensive grinding with KBr results in conversion of the initial spectrum of $Ru_2(AcO)_4Cl$ (Figure 9a), which is identical with that observed in a hydrocarbon mull or a single crystal, to the spectrum shown in Figure 9b. The latter spectrum is probably that of $[Ru_2(AcO)_4Br_2]^-$, for the following reasons.

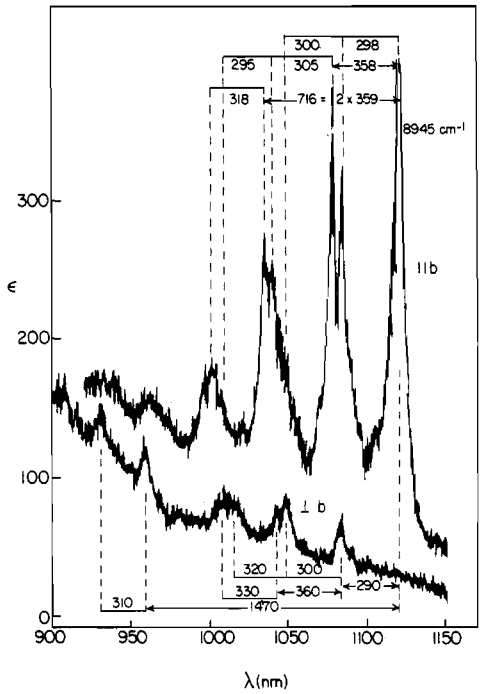

Figure 10. Polarized single-crystal spectra for the (101) face of a $Ru_2(AcO)_4Cl$ crystal at 12 K. The crystal thickness was 9 μm. The maximum of the 0–0 transition was too intense to be recorded with this crystal.

The origin in the spectrum of $Ru_2(AcO)_4Br$ (Table V) is only very slightly shifted from that of $Ru_2(AcO)_4Cl$, in close analogy to the butyrates, while the reaction of $Ru_2(AcO)_4Cl$ with KCl produces an origin near that of $Cs[Ru_2(AcO)_4Cl_2]$. Note that the small but real red shift of the $\delta \rightarrow \delta^*$ transition for discrete $[Ru_2(AcO)_4X_2]^-$ units relative to $[Ru_2(AcO)_4X]_\infty$ chains agrees with our observations on propionates (Table IV). This slight shift is probably due to electrostatic effects.

Although the acetate spectra are grossly similar to those of the other alkanoates, they are different in the sense that there are *two* progression-building frequencies, ~300 and ~360 cm^{-1}. The isotropic spectra (Figure 9) suggest that these two systems have similar Franck–Condon factors. The only other well-defined interval is ~1450-cm^{-1}, attributable to $\nu(CO_2)$.

Polarized single-crystal spectra for the (101) face of monoclinic ($I2/m$) $Ru_2(AcO)_4Cl$ are shown in Figure 10. In this crystal there are linear chains $(Ru_2(AcO)_4Cl)_\infty$ parallel to the crystal *b* axis, with individual Ru_2 units at positions of C_{2h} site symmetry.[10] The $\|b$ and $\perp b$ spectra (Figure 10) are therefore the $\|z$ and $\perp z$ components.

The crystal used to obtain these spectra was rather small, and the data are not of very high quality; in particular, the rising base line at shorter wavelengths is an instrumental artifact (see Experimental Section). Nevertheless, the situation is clearly defined by comparison to Figure 9a. The origin at 8945 cm^{-1} is completely

(37) The observed intensity ratio is somewhat sample dependent, with KBr pellet samples showing ratios near 0.5 vs. 0.65 for single-crystal samples. This may be a crystal-size effect.[36] For a given sample, the intensity ratio of the doublets is independent of temperature over the range 4.9–40 K.

(38) Allen, J. W.; MacFarlane, R. M.; White, R. L. *Phys. Rev.* **1969**, *179*, 523.

(39) The strong visible band also peaks at 480 nm in the CH_3CN solution spectrum of $[Ru_2Prop_4Br_2]^-$.

(40) Yersin, H.; Otto, H.; Zink, J. I.; Gliemann, G. *J. Am. Chem. Soc.* **1980**, *102*, 951.

molecular z polarized, and the z polarization exhibits progressions in both 300- and 360-cm^{-1} vibrational intervals with I_{10}/I_{00} (the Huang–Rhys factor) slightly larger for the 360-cm^{-1} frequency.

The molecular x,y ($\perp b$) spectrum has origins 290 and 1450 cm^{-1} from the 0–0 line. In the case of the 290-cm^{-1} origin, progressions in both 300 and 360 cm^{-1} are built on it, but with Franck–Condon factors very different from those of the $\parallel b$ spectrum, those for the 360-cm^{-1} mode being relatively weaker $\perp b$. Note that the isotropic spectrum, which can be calculated from these data (according to $\epsilon(\text{isotropic}) = {}^1/_3(\epsilon(z) + 2\epsilon(x,y))$, accords with that observed in Figure 9a.

Excited-State Vibronic Assignments and Distortions

Our results establish that the ~1100-nm absorption of the ruthenium carboxylates is a molecular z dipole-allowed transition; this finding and the predominant vibronic involvement of $\nu(Ru_2)$ are consistent with a $\delta \rightarrow \delta^*$ assignment.

For the butyrates and propionates, $\nu(Ru_2)$ dominates the vibronic structure, and the I_{10}/I_{00} intensity ratios are 0.6–0.7. From ground-state and excited-state $\nu(Ru_2)$ values of 330 and 305 cm^{-1}, we calculate (diatomic approximation)[40] that the excited-state Ru_2 bond distance is ~0.05 Å longer than that of the ground state. This is only about half as large as the distortion obtained from an analogous calculation for the $^1(\delta\delta^*)$ state[2a] of $Mo_2(AcO)_4$. The smaller excited-state distortion for the ruthenium complex can be attributed to its longer metal–metal distance. The δ interaction is therefore weaker, and population of the δ^* orbital is of less consequence.

The butyrates and propionates also show vibronic origins at ~430 and ~400 cm^{-1}, respectively, from the origin in their z-polarized spectra. Because of the low Franck–Condon factors, we expect the excited-state frequencies to be close to those of the ground state, and assignment to the a_{1g} ν(RuO) modes is therefore reasonable. The well-resolved butyrate spectra also show a weak vibronic origin at ~700 cm^{-1}, which can be assigned to the a_{1g} $\delta(CO_2)$ vibrational mode. The CO_2 angle in carboxylate-bridged complexes has been shown[15] to be responsive to metal–metal distance, so weak Franck–Condon activity for this mode is reasonable.

The 360-cm^{-1} excited-state progression in the acetates is attributed to a_{1g} ν(RuO). It has suddenly become strongly Franck–Condon active. The excited-state frequency is ~10 cm^{-1} lower than that of the ground state (Table I), a smaller reduction than might have been expected if the large Franck–Condon factors were attributable to changes in RuO distances and force constants. The key factor here is that the a_{1g} ν(RuO) and $\nu(Ru_2)$ modes are coupled in the ground states of the acetates, and the Franck–Condon activity of ν(RuO) reflects this coupling. Since the frequency difference of two vibrations is greatly increased in the excited state, we expect that they should be essentially decoupled. The 10-cm^{-1} change in the excited-state frequency probably reflects this decoupling. In other words, we infer a very large Duschinsky effect[41] for the excited state. It may be relevant to note here that Clark et al.[18b] explicitly mentioned that this effect possibly is involved in resonance Raman intensities for visible excitation (of a completely different electronic transition) of ruthenium carboxylates. Since the latter transition also should lead to a large change in RuRu bond length,[18b,31] excited-state decoupling of $\nu(Ru_2)$ and ν(RuO) could again occur.

A Duschinsky effect could be confirmed[42] if the vibronic intensities were compared for $\delta \rightarrow \delta^*$ absorption and $\delta^* \rightarrow \delta$ emission. Unfortunately, the electronic emission in question would fall in a wavelength region that is very difficult to probe experimentally. We emphasize, however, that there is good evidence for ground-state coupling of $\nu(Ru_2)$ and ν(RuO) for the acetates and that this coupling explains the strong Franck–Condon activity of a_{1g} ν(RuO).

It is apparent that the a_{1g} δ(RuO) and ν(RuX) modes are not strongly coupled to the electronic transition. However, these modes could be responsible for some very weak absorption features with 200–100-cm^{-1} frequency differences from the electronic origin. The relatively weak activity does not imply that Ru_2O bond angles and RuX bond distances are unaffected in the excited state; indeed, both parameters are coupled to the RuRu bond distance and therefore must be involved in the $\nu(Ru_2)$ normal mode. Moreover, since these two vibrational modes are low frequency (high amplitude) relative to $\nu(Ru_2)$, their Franck–Condon intensities should be low unless distortions along their normal coordinates are relatively large compared to that along the metal–metal coordinate.

The z-polarized component of the $\delta \rightarrow \delta^*$ transition of $Mo_2(AcO)_4$[2a] and related compounds[2b] is similar to that of the ruthenium carboxylates in that it shows predominant Franck–Condon activity for $\nu(M_2)$, weak activity for a frequency attributable to a_{1g} ν(MO) (~320 cm^{-1} for Mo_2Ac_4),[2a] and very weak activity for other vibrational modes.

Consider now the molecular x,y-polarized absorption. It has been shown[2] that the $\delta \rightarrow \delta^*$ transitions of compounds with quadruple metal–metal bonds often include strong vibronically allowed x,y-polarized components,[2,3] and there is reason to believe that the x,y-polarized absorption in the present case should be similarly assigned. First, both z- and x,y-polarized absorptions exhibit progressions in the same frequencies: ~300 cm^{-1} for propionates and butyrates and ~300 and ~360 cm^{-1} for acetates. Secondly, in the set of compounds we have investigated, the electronic origin varies over a range of 300 cm^{-1}, and the x,y-polarized origins shift as the z-polarized origin does. Finally, and most importantly, the x,y-polarized lines of $I\bar{4}2d$ Ru_2But_4Cl all show the same factor group splitting as the z-polarized lines (Figure 7). Thus, an interpretation of the x,y-polarized absorption (or part of it) in terms of another electronic transition would require an unlikely set of coincidences.

Interpreting the x,y-polarized absorption as a vibronically induced component of the $\delta \rightarrow \delta^*$ transition requires that it be built on vibrations of e_g (D_{4h}) symmetry. (Note that the participation of e_u vibrations is rigorously excluded for the C_{2h} site symmetry of $Ru_2(AcO)_4Cl$.) Three x,y-polarized origins are evident in our data: a weak one at ~250 cm^{-1}, which is clearly defined only for the butyrates, and stronger ones at ~310 and ~1450 cm^{-1}. The first of these is assigned to an e_g RuO_2 deformation mode, and the last to the e_g antisymmetric CO_2 stretch[43] (vide supra). The ~310-cm^{-1} origin has troubled us, since it coincides roughly with the excited-state a_{1g} $\nu(Ru_2)$ frequency. Earlier we suggested that a ground-state ν(RuO) mode is near 300 cm^{-1}, which might be the e_g mode and which would nicely account for the absorption spectra. While this explanation requires a near coincidence of a_{1g} $\nu(Ru_2)$ and e_g ν(RuO) in the excited state, there does not appear to be a reasonable alternative explanation.

It is interesting to compare these presumed e_g vibrational modes to those observed for the $\delta \rightarrow \delta^*$ transition of $Mo_2(AcO)_4$, where x,y-polarized origins at 255 and 275 cm^{-1} are possibly due to e_g $\delta(MoO_2)$ and ν(MoO) modes. However, the strongest x,y-polarized vibronic origin for $Mo_2(AcO)_4$ has a frequency[2a,44] of 545 cm^{-1}. Such a frequency may be assigned to a CO_2 rock;[23,26] there does not appear to be an analogue in our spectra, while our 1450-cm^{-1} mode apparently is absent in the $Mo_2(AcO)_4$ case.

According to the conventional Herzberg–Teller coupling scheme, the intensities of the nontotally symmetric vibronic origins reflect geometry changes (Franck–Condon factors) in the electronic transitions from which x,y-polarized intensity is being stolen. For both dimolybdenum[2] and diruthenium[10,29] carboxylates, the lowest energy intense x,y-polarized electronic transitions fall in the ultraviolet and probably involve metal–carboxylate charge transfer,[4] so the activity of CO_2 rocks or stretches is reasonable. The relatively small[2] vibronic x,y intensity of $\delta \rightarrow \delta^*$ for the ruthenium complexes is explicable on the basis of a larger energy

(41) Duschinsky, F. *Acta Physicochim. URSS* **1937**, *1*, 551.
(42) Small, G. J. *J. Chem. Phys.* **1971**, *54*, 3300.
(43) We can rigorously eliminate the possibility that this frequency might be due to a methylene deformation mode; the 15 K $\delta \rightarrow \delta^*$ absorption band of Ru_2Form_4Cl (hydrocarbon mull) shows[31] a strong vibronic origin 1490 cm^{-1} from its electronic origin.
(44) Manning, M. C.; Trogler, W. C. *Inorg. Chem.* **1982**, *21*, 2797.

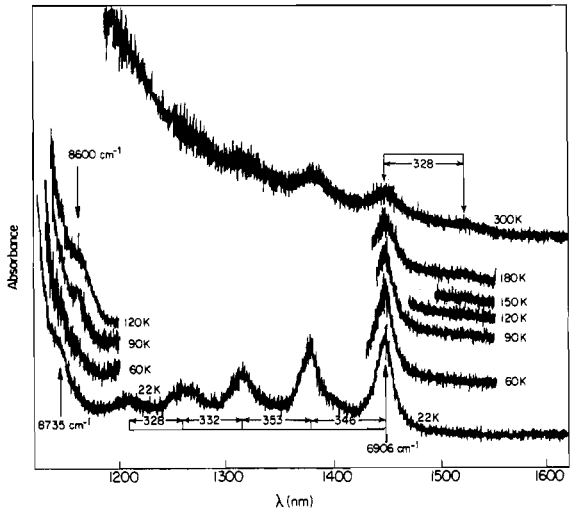

Figure 11. Temperature dependence of the absorption spectrum of a concentrated (35 mg/170 mg of KBr) KBr pellet of $Ru_2(AcO)_4Cl$. The weak low-temperature absorption shoulder at 8735 cm^{-1} is the $\delta \rightarrow \delta^*$ origin of a trace of $[Ru_2(AcO)_4Br_2]^-$ in this sample, while the ~8600-cm^{-1} hot band is the $[\nu(Ru_2), \nu(RuO)]$ hot band of the $\delta \rightarrow \delta^*$ transition of $Ru_2(AcO)_4Cl$.

gap, while the different allowed modes may reflect differences in the coupled charge-transfer states.

A result of special interest is that the Franck–Condon factors for $\nu(Ru_2)$ are very different for the z and x,y components of absorption. This sort of effect has been noted before for $\delta \rightarrow \delta^*$ transitions[2,3] and explained in terms of vibronic coupling via totally symmetric[45] vibrations; according to this theory, the Franck–Condon factors for the molecular z-polarized component of the absorption are affected by coupling[45,46] to other z-polarized transitions.

An alternative view would ascribe[47] the deviant Franck–Condon factors to the x,y polarization, which would be modified by interaction with some x,y-polarized state(s) of different equilibrium RuRu distance. While none of our results excludes important coupling effects in z polarization, we do see definite evidence for coupling in x,y polarization. Consider Figure 5: the I_{10}/I_{00} ratio for the $\nu(Ru_2)$ progression based on the 310- and 245-cm^{-1} vibronic origins is 1.4, but only about 1.0 for the progression built on the 1445-cm^{-1} vibronic origin. Very similar intensities are evident in Figure 7 and in our other data. Thus, not only are the $\nu(Ru_2)$ Franck–Condon factors for x,y polarization different from those of z polarization, but they are also different for the various x,y-vibronic origins.

A possible explanation is that the various e_g vibrations couple the $\delta \rightarrow \delta^*$ state to different x,y-polarized transitions. Alternatively, the dispersion in Franck–Condon factors could be due to coupling to one nearby x,y-polarized electronic transition;[47] small changes in the energy gap would then have a marked effect on vibronic intensities. This transition could not be one from which x,y intensity is being stolen, as there are no nearby intense x,y-polarized transitions.[10,29] However, a coupled transition can have large effects on vibronic intensities even if it carries no inherent intensity.[48] We will show below that there is at least one spin-forbidden but x,y-dipole-allowed transition very near the $\delta \rightarrow \delta^*$ transition, and coupling to this transition may be involved.

Spin-Forbidden Transitions

Next we consider transitions from the high-spin (quartet) ground state to doublet $(\pi^*,\delta^*)^3$ excited levels. Comparison to $4d^3$ Mo(III) complexes indicates that these quartet–doublet transitions should appear in the infrared to near-infrared region.[49]

There are two $(\pi^*,\delta^*)^3$ excited states of ^2E_g symmetry. Transitions to these states from the $^4B_{2u}$ ground state are x,y dipole allowed; if the two ^2E_g states do not interact, the excitations are simply $\delta^* \rightarrow \pi^*$ and $\pi^* \rightarrow \delta^*$. In addition, there are four excited states, $^2A_{2u}$, $^2B_{2u}$, $^2A_{1u}$, and $^2B_{1u}$ (D_{4h} labels), which are formed by spin flips. Transitions to the spin-flip states are all both spin and dipole forbidden; they are expected to give rise to sharp but very weak bands in absorption.

Absorption spectra for a very concentrated KBr pellet of $Ru_2(AcO)_4Cl$ are shown in Figure 11. A nicely structured but extremely weak absorption band (isotropic $\epsilon \sim 2$, assuming Beer's law to hold for KBr pellets) is evident, with an electronic origin at 6906 cm^{-1}, about 3000 cm^{-1} below the electronic origin of the spin-allowed $\delta \rightarrow \delta^*$ transition. No other absorption is observed in the near-infrared region that cannot be assigned to vibrational overtones by comparison to near-infrared spectra of copper(II) and rhodium(II) acetates. (We have measured near-infrared spectra out to 2700 nm.)

The first two intervals in the progression are ~350 cm^{-1}; further intervals are somewhat smaller (Figure 11), but distinctly broader lines suggest that other vibronic origins may be contributing to absorption here. Figure 11 also indicates that a hot band is observed ~330 cm^{-1} to the red of the origin line. So we attribute the progression frequency to $\nu(Ru_2)$.

Very similar absorption bands are observed for the other ruthenium carboxylates (Table VI), with simple progressions observed in frequencies of 330–350 cm^{-1}. We have had difficulty obtaining single crystals thick enough to observe these weak bands. As indicated in Table VI, we did see the band in axial spectra of Ru_2Prop_4Cl and Ru_2But_4Br; the observed extinction coefficients

Table VI. Low-Temperature $\pi^* \rightarrow \delta^*$ Absorption Parameters for Ruthenium Carboxylates

	electronic origin, cm^{-1}	extinction coefficient
$I4/m$ Ru_2Prop_4Cl	6950	3[a]
$4/m$ Ru_2But_4Cl	6940	~3[c]
$4/m$ Ru_2But_4Br	6800	4[a]
$I2/m$ $Ru_2(AcO)_4Cl$	6906	~2[c]
$I\bar{4}d$ Ru_2But_4Cl	6854	2[b]

[a] Axial crystal face. [b] ϵ approximately 2 both $\|c$ and $\perp c$. [c] KBr pellet.

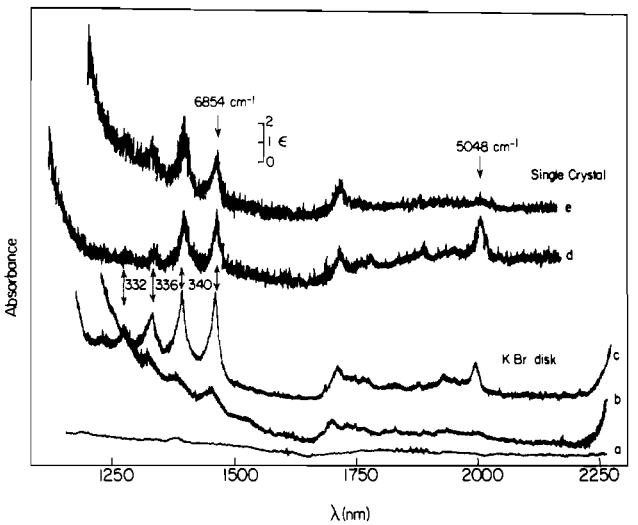

Figure 12. Absorption spectra of the $I\bar{4}2d$ polymorph of Ru_2But_4Cl: (a) KBr pellet absorption baseline; (b and c), 53.1 mg of Ru_2But_4Cl/200 mg of KBr, spectra at 300 and 18 K, respectively; (d and e), single-crystal spectra at 20 K, $\|c$ and $\perp c$, respectively. The single crystal was 400-μm thick and an extinction coefficient scale is included near the top of the figure.

(45) Craig, D. P.; Small, G. J. *J. Chem. Phys.* **1969**, *50*, 3827.
(46) Gregory, A. R.; Hennecker, W. H.; Siebrand, W.; Zgierski, M. S. *J. Chem. Phys.* **1977**, *67*, 3175.
(47) Gregory, A. R.; Siebrand, W.; Zgierski, M. S. *J. Chem. Phys.* **1976**, *64*, 3145.
(48) Hochstrasser, R. M.; Marzacco, C. *J. Chem. Phys.* **1968**, *49*, 971.
(49) Stiefel, E. I. *Prog. Inorg. Chem.* **1977**, *22*, 1.

are similar to isotropic values, so the transition is certainly not z polarized. Polarized data could only be obtained for the $I\bar{4}2d$ polymorph of Ru_2But_4Cl (Figure 12).

The band appears to be of roughly equal intensity ($\epsilon \sim 2$) both $\parallel c$ and $\perp c$. Again, it is clearly not z polarized. If it were molecular x,y polarized, we would expect in the oriented gas approximation that the absorption intensity $\parallel c$ would be just twice that $\perp c$. Since the site symmetry is low, we consider our observations to be consistent with an x,y-polarized transition. Note that the temperature dependence of the band (Figures 11 and 12) is consistent with a dipole-allowed transition.

We therefore assign the band in question to a transition to one of the ^2E_g excited states. The $\nu(Ru_2)$ appears to be slightly larger than in the ground state, so the one-electron assignment $\pi^* \rightarrow \delta^*$ is reasonable. If we take the excited- and ground-state $\nu(Ru_2)$ frequencies to be 340 and 330 cm^{-1}, respectively, then the I_{10}/I_{00} intensity ratios of $\sim$1 are consistent[40] with an excited-state RuRu distance that is $\sim$0.06 Å shorter than that in the ground state.

The temperature dependence of this absorption band is very different from that of the $\delta \rightarrow \delta^*$ transition. While limiting low-temperature vibronic line widths are about twice as large as for $\delta \rightarrow \delta^*$, much less broadening occurs at higher temperatures. Perhaps this reflects opposite excited-state metal–metal bond distance changes; metal–halide deformations are probably involved in the $\delta \rightarrow \delta^*$ temperature dependence, and the chromophore may be insensitive to these modes if it does not increase its metal–metal bond length in the excited state.

Factor group splitting was not observed for the $\pi^* \rightarrow \delta^*$ absorption of the $I\bar{4}2d$ form of Ru_2But_4Cl (Figure 12). This is reasonable, in view of the extreme weakness of the transition, according to electric dipole coupling models.[37]

There are two absorptions that are candidates for spin-flip transitions. One of them is a sharp line at 5048 cm^{-1} (Figure 12). There is no analogous line in the near-infrared absorption spectra of the other compounds; most importantly, the spectrum of the $4/m$ polymorph of Ru_2But_4Cl does not show it. The single-crystal spectra establish that it is completely polarized $\parallel c$ ($\epsilon \sim 2$); this result suggests that the absorption is attributable to a forbidden electronic transition that has become allowed in the low site symmetry lattice of the $I\bar{4}2d$ polymorph, as pure polarization $\parallel c$ is not explicable on the basis of an oriented gas model in this lattice. It also shows high-temperature broadening (Figure 12b,c) that is much more drastic than that of absorption features attributable to vibrational overtones such as the $\sim$1750-nm cluster of lines (the third overtone of $\nu(CO_2)$, methylene deformation fundamentals at $\sim$1450 cm^{-1}). While some of the absorptions to higher energy of the 5048-cm^{-1} line might be due to vibronic side bands, they are clearly much weaker than the origin; the transition in question is vertical.

Among the various spin-flip transitions, two of them become allowed $\parallel c$ (parallel to the site C_2 axis) in the $I\bar{4}2d$ lattice; these are the transitions to $^2B_{2u}$ and $^2A_{1u}$ excited states, which are therefore possible assignments for the 5048-cm^{-1} absorption.

A second spin-flip transition is suggested from the Raman work of Clark et al.,[18] who observed Raman peaks at (low-temperature values[18b]) 1582 cm^{-1} for Ru_2But_4Cl and 1591 cm^{-1} for Ru_2Prop_4Cl. Our present vibrational analysis does not place CO stretching fundamentals near 1600 cm^{-1}. More importantly, the observed "ν(CO)" bands have half-widths of 100–200 cm^{-1} (see Figure 3 of ref 18a and Figure 7 of ref 18b). This is extraordinarily broad for a vibrational transition but reasonable for a vertical electronic transition. We therefore suggest reassignment to an electronic Raman transition.[50]

The proposed spin-flip Raman peak shows resonance enhancement,[18] indicative of a totally symmetric transition. The simplest assignment would then be the $^4B_{2u} \rightarrow {}^2B_{2u}$ spin flip. There is a complication, however. Other ruthenium carboxylates do not show strictly analogous Raman features: while $Ru_2(AcO)_4Cl$ reportedly exhibits a weak $\sim$1600-cm^{-1} line at room temperature, the feature vanishes at low temperature.[18b] This suggests that the transition is not inherently allowed (perhaps it is allowed at high temperature by a vibronic mechanism) but becomes totally symmetric in the Ru_2But_4Cl and Ru_2Prop_4Cl lattices. Clark et al.[18] appear to have studied the $I\bar{4}2d$ polymorph of the butyrate. The propionate was presumably the material that crystallizes from propionic acid, whose structure has not been established. For the $I\bar{4}2d$ butyrate, the $^4B_{2u} \rightarrow {}^2B_{2u}$ and $^2A_{1u}$ transitions become totally symmetric; thus, we place one of them at 1582 cm^{-1} and the other at 5048 cm^{-1}.

Acknowledgment. We thank R. E. Marsh and S. F. Rice for helpful discussions and D. S. Martin and R. J. H. Clark for communication of results prior to publication. This research was supported by National Science Foundation Grant CHE84-19828.

(50) (a) Clark, R. J. H.; Dines, T. J. *Adv. Infrared Raman Spectrosc.* **1982**, *9*, 282. (b) Larrabee, J. A.; Spiro, T. G. *J. Am. Chem. Soc.* **1980**, *102*, 4217.

Contribution No. 7455 from the Arthur Amos Noyes Laboratory, California Institute of Technology, Pasadena, California 91125

Electronic Spectra of Tetranuclear Linear-Chain Rhodium Isocyanide Complexes

Vincent M. Miskowski* and Harry B. Gray*

Received August 20, 1986

The electronic spectrum of the tetranuclear rhodium complex $Rh_4b_8^{6+}$ (b = 1,3-diisocyanopropane) has been studied as a function of medium and temperature. The intense absorption at $\sim$600 nm is attributed to a $\sigma \rightarrow \sigma^*$ transition within the linear Rh_4^{6+} unit. Both band-moment studies and a simple Hückel model for the metal–metal bonding indicate that the excited-state distortion is confined to an elongation of the central metal–metal bond.

A tetranuclear rhodium complex, $Rh_4b_8^{6+}$ (b = 1,3-diisocyanopropane), has been found[1] to react photochemically with protons to produce H_2. The $CoCl_4^{2-}$ salt of $Rh_4b_8^{6+}$ contains a Rh_4^{6+} linear chain with a central Rh–Rh length of 2.775 Å and outer Rh–Rh distances of 2.932 and 2.923 Å.[2] The central bond length is similar to single-bond distances found in binuclear Rh_2^{4+} (d^7–d^7) complexes of isocyanide ligands, whereas the outer bond

(1) (a) Miskowski, V. M.; Sigal, I. S.; Mann, K. R.; Gray, H. B.; Milder, S. J.; Hammond, G. S.; Ryason, P. R. *J. Am. Chem. Soc.* **1979**, *101*, 4384–4385. (b) Mann, K. R.; Gray, H. B. *Adv. Chem. Ser.* **1979**, *No. 173*, 225–235. (c) Mann, K. R.; Lewis, N. S.; Miskowski, V. M.; Erwin, D. K.; Hammond, G. S.; Gray, H. B. *J. Am. Chem. Soc.* **1977**, *99*, 5525–5526.

(2) Mann, K. R.; DiPierro, M. J.; Gill, T. P. *J. Am. Chem. Soc.* **1980**, *102*, 3965–3967.

(3) (a) Rice, S. F.; Gray, H. B. *J. Am. Chem. Soc.* **1981**, *103*, 1593–1595. (b) Rice, S. F. Ph.D. Thesis, California Institute of Technology, 1982.

0020-1669/87/1326-1108$01.50/0